

## Original Article

# A new crystal form of mouse thiamin pyrophosphokinase

Jing-Yuan Liu, Thomas D. Hurley

Department of Biochemistry and Molecular Biology, Indiana University School of Medicine, Indianapolis, IN 46202, USA.

Received February 22, 2011; accepted February 26, 2011; Epub February 28, 2011; Published April 30, 2011

**Abstract:** Thiamin pyrophosphokinase (TPK) transfers a pyrophosphate group from ATP to the hydroxyl group of thiamin and produces thiamin pyrophosphate (TPP). TPP is the cofactor of metabolically important enzymes such as pyruvate dehydrogenase,  $\alpha$ -ketoglutarate dehydrogenase, branched-chain  $\alpha$ -keto acid dehydrogenase, transketolase and 2-hydroxyphytanoyl-CoA lyase. Thiamin deficiency results in Wernike-Korsakoff Syndrome (WKS) due to neurological disorder and wet beriberi, a potentially fatal cardiovascular disease. Mouse TPK associates as a dimer revealed by previous solved crystallographic structures. In this study, we report mouse TPK complexed with TPP-Mg<sup>2+</sup> and thiamin-Mg<sup>2+</sup>, respectively, in a new crystal form. In these two structures, four mouse TPK molecules were found in each asymmetric unit. Although we cannot rule out this tetramer form can be an artifact from crystal packing, mouse TPK tetramer has a more closed ATP binding pocket and has the potential to provide specific interactions between mouse TPK and ATP compared with the previous dimeric structure and is likely to be an active form.

**Keywords:** Thiamin pyrophosphokinase (TPK), crystal structure, TPP-Mg<sup>2+</sup>, thiamin-Mg<sup>2+</sup>, protein oligomerization, dimer, tetramer

## Introduction

Thiamin pyrophosphokinase (TPK; EC 2.7.6.2) is a member of the pyrophotransferase family. It catalyzes the transfer of a pyrophosphate group from ATP to thiamin to form thiamin pyrophosphate (TPP). The product, TPP, is a cofactor for the reactions catalyzed by pyruvate dehydrogenase,  $\alpha$ -ketoglutarate dehydrogenase, branched chain  $\alpha$ -keto acid dehydrogenase, transketolase and 2-hydroxyphytanoyl-CoA lyase. Thus, TPP plays a central role in carbohydrate metabolism and TPK activity is critical to the cellular energy generation. In addition to TPP, thiamin monophosphate (TMP) and thiamin triphosphate (TTP) are also found in human cells. Among thiamin and its phosphoesters, TPP is the major form [1, 2] and plays a central role in thiamin phosphoester synthesis. Following thiamin transport into cells, it is converted to TPP by TPK in the cytosol very rapidly; after that, TMP and TTP can be synthesized from TPP [3-5].

The catalytic parameters of TPK purified from various species and tissues have been charac-

terized. The  $K_m$  of mammalian TPK for thiamin is close to physiological levels while  $K_m$  for MgATP was found to be extremely high ranging from 59mM to 3mM [6-8]. Onozuka M and Nossaka K. determined the  $K_m$  for MgATP with purified recombinant human TPK to be 1.2 mM at a later time, which is probably more reasonable regarding its physiological function [9]. Previously, we have solved crystal structures of mouse TPK, which shares 89% sequence identity to human TPK [10]. The TPK polypeptide consists of an  $\alpha/\beta$ -domain and a  $\beta$ -sandwich domain. Mouse TPK associates as a dimer and thiamin is found in the dimer interface. The structure of TPP bound mouse TPK was solved subsequently and TPP adopts an F-conformation in mouse TPK, which is different from the V-conformation seen in the enzymes that recruit TPP as cofactor [11]. In addition, we further demonstrated that pyridoxal, an inhibitor of TPK that can induce WK syndrome in animals, is a substrate of TPK and can be phosphorylated [12]. Pyridoxal pyrophosphate (PPP) along with Mg<sup>2+</sup>/AMP is located in the active site of the enzyme. In the above structures, mouse TPK exists as dimers. In this study,

**Table 1.** Crystallographic data and refinement statistics

Data sets	TPP-Mg-mouse TPK	Thiamin-Mg-mouse TPK
Data collection		
Wavelength (Å)	0.9	
Space group	P2 <sub>1</sub>	
Resolution (Å)	2.76	2.42
Cell constants		
a, b, c (Å)	75.38, 94.83, 83.8590	75.54, 95.21, 84.2790
a, b, g (°)	105.3, 90	105.2, 90
Measured reflections	99673	164426
Unique reflections	27991	43925
Completeness (%)	96.7	99.9
R <sub>sym</sub> (%)	12 (45.6)	12.4 (37.8)
Refinement		
R <sub>work</sub> / R <sub>free</sub> (%)	22.1 (22.4)	21.9 (22.6)
Number of atoms/AU	8233	8359
Nonhydrogen atoms	8233	8359
Solvent molecules	280	442
RMSD		
Bond length (Å)	0.013	0.011
Bond angles (°)	1.8	1.6

we report a new crystal form of mouse TPK, in which each asymmetric unit contains four sub-units of mouse TPK.

## Materials and methods

### Protein purification and crystallization

Mouse TPK cDNA was cloned in pET28a vector (Novagen) for expression as a His-tagged protein in BL21 cells. The transformed cells were cultured in TY media at 37°C until the OD<sub>600</sub> reached between 0.8 and 1.0. IPTG was then added to a final concentration of 70mg/mL and the culture was incubated at room temperature for an additional 12 to 15 hours. Cells were collected by centrifugation and were lysed using a French Press. The recombinant mouse TPK was purified by nickel-chelate chromatography and analyzed by SDS-PAGE as previously described [10].

Purified recombinant mouse TPK was sequentially dialyzed against three buffers: (1) 5 mM EDTA, 150 mM NaCl, 50 mM Tris, pH7.5; (2) 1 mM EDTA, 150 mM NaCl, 50 mM Tris, pH7.5; and (3) 150 mM NaCl. Dialyzed protein was then concentrated to 12 mg/mL using a Centri-

con concentrator. Crystals are yielded at room temperature in condition 1.15-1.3M sodium citrate, 0.1M NaHepes, pH 8.6 utilizing hanging drop vapor diffusion geometry.

### Data collection, processing and structure determination

For the TPP-Mg<sup>2+</sup>-complexed structure, crystals were soaked with 20mM TPP and 0.1M MgAMP, pH7.0 for 2 hours before data collection. For thiamin-Mg<sup>2+</sup> complexed structure, crystal was soaked with 10mM thiamin and 0.1M AMPCPP, pH7.0. Crystals were cryo-protected in 15% glycerol. Both data sets were collected at Argonne National Laboratory BioCARS 14BM-C. The raw intensity data were merged and scaled by HKL2000 [13]. The intensity output was converted into structure factors using the program package CCP4 [14]. Molecular replacement was done using the initial phase information from the mouse TPK dimeric structure by CNS (v1.0) [15]. Models were manually adjusted in program O and refined by CNS (v1.0). Thiamin and TPP coordinates were acquired as previously described [10, 11]. Statistics for crystallographic data and refinement are shown in **Table 1**.

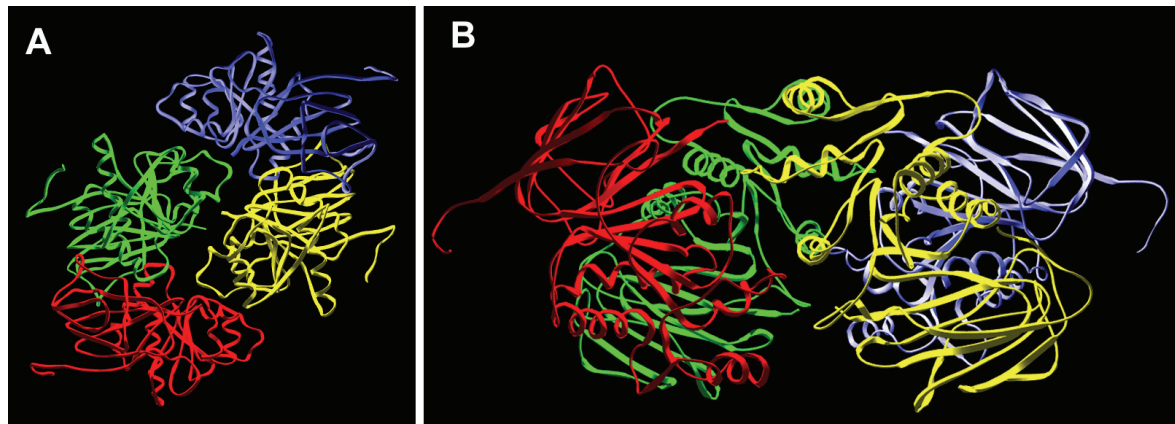


**Figure 1.** The overall structure of mouse TPK tetramer. **A.** A view of the tetramer structure parallel to its two fold axis. **B.** A view of the tetramer structure perpendicular to its two fold axis. The four subunits assigned as A, B, C and D are colored in green, red, yellow and blue, respectively. A and B or C and D form the previously described U-shaped dimer unit.

## Results

### The overall structure

A new crystal form of mouse TPK with P2<sub>1</sub> space group was acquired. Structures of mouse TPK complexed with TPP-Mg<sup>2+</sup> and thiamin-Mg<sup>2+</sup> in this new crystal form were solved by crystal soaking experiment at resolution 2.7 Å and 2.4 Å, respectively. In the new crystal form, the asymmetric unit contains a tetrameric TPK, which consists of two protein dimers. Each dimer component roughly keeps its general U-shaped structure described in the P3<sub>1</sub>21 space group [10] with shifts in some secondary structural elements. The RMSD of all atoms (side chain and main chain) and main chain atoms only between one dimer component of the tetramer and the previously solved dimer is 0.909 Å and 0.495 Å, respectively. The four chains assigned as A, B, C and D, in which sub-unit A and B or C and D form the original dimeric unit, are shown in green, red, yellow and blue, respectively (Figure 1). The two U-shaped dimers are arranged as that the arm of one U is embedded in the cleft of the other and forms an overall structure similar to an interlocked two crescents when viewed parallel to its 2-fold axis. Residues 13 to 16, 37 to 38, 57 to 59 and 60 to 62 of subunit A interact with residues 76 to 78, 51 to 57, 158 to 160 and 27 to 31 of sub-unit D, respectively. In addition, subunit A also interacts with subunit C mainly through residues 54 to 55, 25 to 27, and residue 243 with that of

25 to 27, 55 to 57, and residue 243 of the C subunit, respectively. While subunit A interacts with both subunits of the opposite dimer, sub-unit B interacts with subunit C only. Intensive interactions are between residues 27 to 31, 53 to 57, and 76 to 78 of B subunits and residues 59 to 61, 37 to 38, and 13 to 16 of the C sub-unit, respectively. Moreover, residue 242 and 243 at the C-terminus of B subunit interacts with residue 82 and 86 of C subunit.

Structural changes accommodating the new comer of another dimeric protein in the tetrameric structure are mostly located either on loops or at the end of helices. For example, the loop containing residues 52 to 58 on the A subunit shifted toward A subunit itself to make room for the joining of C and D subunit. Most of the residues in the dimer-dimer interface have conformational changes, which can be on either side chain or main chain or both. The most special one is the C-terminal residue Ser243. The C-terminus points to a different direction from that of the dimeric structure (Figure 2A). The arrangement of the tetramer and the movement of C-terminus brought Ser243 on A and C sub-unit close to each other. As a result, the distance between the hydroxyl oxygen of Ser243 of A subunit and the main chain carbonyl oxygen of Ser243 of C subunit is 2.93 Å (Figure 2B). However, Ser243 of subunit B and D are not close because only one fold symmetry is found in the tetrameric structure. Instead, Ser243 of B and D subunit is pushed close to residue Glu61

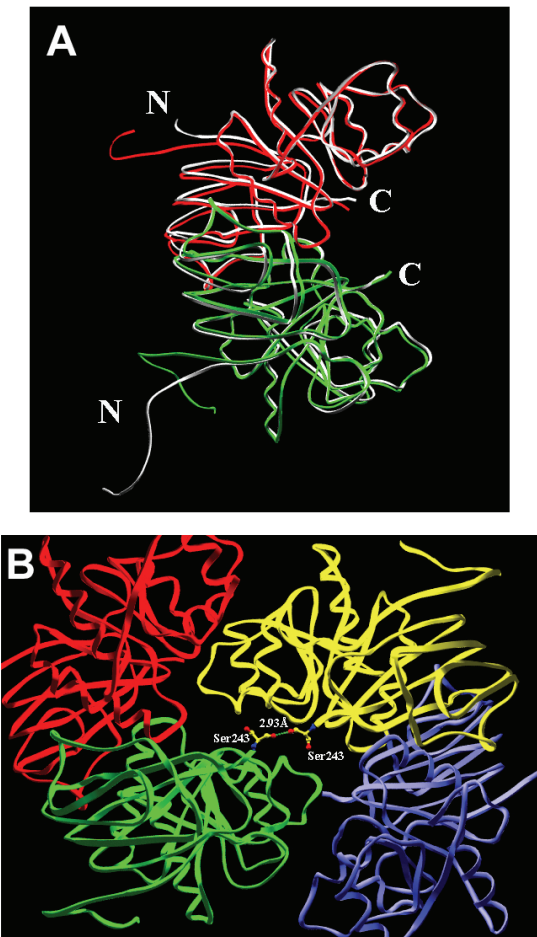


**Figure 2.** Differences between a dimer unit of the tetrameric structure and the dimeric structure of mouse TPK. **A.** Superposition of mouse TPK dimer (in gray) and tetramer (in green and red). The N-terminal His tags are oriented differently and the C-termini are pointed to different directions compared with the dimeric structure. **B.** A zoom in picture of the two C-terminal Ser in A and C subunits. The arrangement of the tetramer and the shift of the C-terminal residue, Ser243, of A and C subunit brought the two residues close enough to form a hydrogen bond between the hydroxyl oxygen of Ser in A subunit and the carbonyl oxygen of Ser in C subunit.

and Lys86 of A and C subunits, respectively.

Residues in the dimer interface between two monomers in the original dimer structure and residues in the dimer-dimer interfaces between two dimer units are located in different domains; the former are mainly located in the  $\beta$  roll domain at C-terminus while the latter are

located mostly in the  $\alpha/\beta$  sandwich domain at the N-terminus. However, Asp159 on B and D subunits can be found in both kinds of interfaces.

In addition to the changes related to tetramer formation of mouse TPK, the conformation of the His tags at the N-terminus are different from the dimeric structure and the His tags are more ordered (**Figure 2A**). The four His tags are not identical. His tags on subunit A and C are similar, and His tags on subunit B and D are similar.

#### The dimer-dimer interface

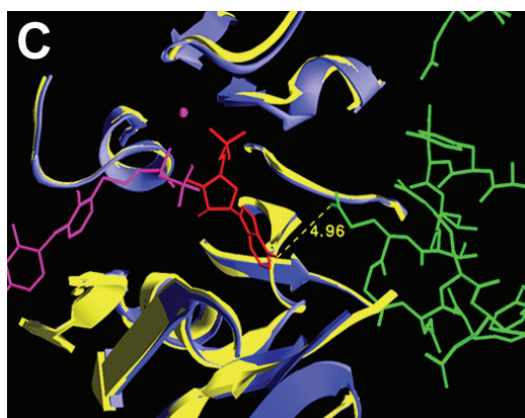
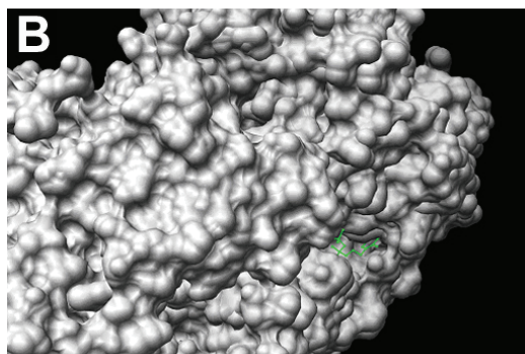
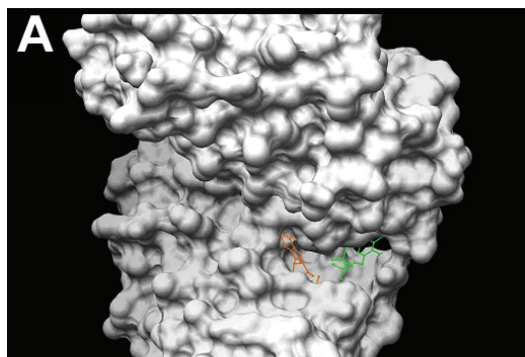
The buried surface area between the interface of the two dimers is  $3191 \text{ \AA}^2$ , which is about 18% of the total accessible surface area of a dimer if His tags are not included. Eleven hydrogen bonds between the two dimer units are found (**Table 2**). Altogether 78 residues including 10 arginines are located in the dimer-dimer interface. Arginine residue has been found statistically to be the second most abundant residues in protein oligomeric interfaces and functions to form hydrogen bonds [16]. In mouse TPK, 5 of the 10 arginine residues are involved in hydrogen bonding directly with residues from opposite dimer, while one of them form hydrogen bond across the interface via a water molecule.

#### The more closed active site

In the tetramer structure, the joining of a second dimer helps to form a less solvent exposed active site. A fairly solvent exposed active site is seen in the dimeric ternary complex of mouse TPK with PPP and MgAMP. The nucleotide binds to the protein loosely due to the fact of the high B factor for AMP in the 'A' subunit of TPK and the mixed occupancy of HEPES and AMP in the 'B' subunit [12]. **Figure 3A** shows the molecular surface of the dimer mouse TPK in complexed with PPP-MgAMP and the solvent exposed binding groove for PPP and MgAMP. The opening of the binding groove might be important for products release and substrates binding. However, for an enzyme with high reaction specificity and efficiency, this opening is likely to be sealed following substrates binding. In the tetramer form of mouse TPK, the way the two dimer units associate with each other provide a more closed binding groove (**Figure 3B**). In addition, the tetrameric structure has potential to provide

**Table 2.** Hydrogen bonds between residues across the dimer interface

Residues and atoms on dimer AB				Residues and atoms on dimer CD			Distance	
Chain	Residue	Atom	Chain	Residue	Atom			
A	13	PRO	O	D	76	ARG	NH1	3.07
A	58	GLY	O	D	159	ASP	N	3.24
A	61	GLU	OE2	D	31	ARG	NH2	2.99
A	62	SER	OG	D	30	ALA	N	3.16
A	76	ARG	NH1	C	76	ARG	NH1	2.78
A	243	SER	OG	C	243	SER	OT	2.93
B	29	ASP	OD1	C	62	SER	OG	3.08
B	30	ALA	N	C	62	SER	OG	3.08
B	76	ARG	NH2	C	13	PRO	O	3.19
B	78	GLU	OE2	C	14	THR	OG1	2.99
B	159	ASP	N	C	58	GLY	O	3.29



specific interactions between mouse TPK and the adenine ring of the nucleotide. Superposition of the tetramer mouse TPK onto the dimeric ternary structure shows that the carboxyl oxygen of Glu57 in subunit C is only 4.96 Å away from the N6 atom of AMP (Figure 3C). Slight conformational change with the side chain of Glu57 can bring the carboxyl oxygen close enough to form a hydrogen bond with the adenine ring. Therefore, the tetramer structure can potentially lower the  $K_m$  between the protein and the nucleotide substrate.

#### Ligand binding

TPP is localized in all of the four subunits of mouse TPK tetramer structure. TPP binds in a similar way as that in the dimeric structure in F conformation [11].  $Mg^{2+}$  was identified in adja-

**Figure 3.** Molecular surface of the dimeric and tetrameric structures. **A.** Molecular surface of the dimeric ternary complex of mouse TPK with PPP-MgAMP. AMP is shown in orange. PPP is shown in green. The binding groove is open to the solvent. **B.** The tetramer mouse TPK is superimposed with the dimer structure and the molecular surface is shown. The joining of another dimer unit helps to seal the active site. **C.** Glu57 may provide additional hydrogen bond across the two dimer interface in the tetrameric structure when nucleotide is bound. The dimeric PPP-MgAMP mouse TPK complex is superimposed onto the tetrameric structure. PPP and  $Mg^{2+}$  are shown in magenta. AMP is shown in red. Distance is shown in angstrom. The dimer structure is shown in yellow; the A and C subunits of the tetramer structure are shown in blue and green. The common part of the two structures is illustrated by ribbon diagram. The C subunit of tetramer, which does not exist in the dimer structure, is in stick presentation. Glu57 in tetramer is 4.96 Å away from the N6 atom of AMP in the dimer structure.

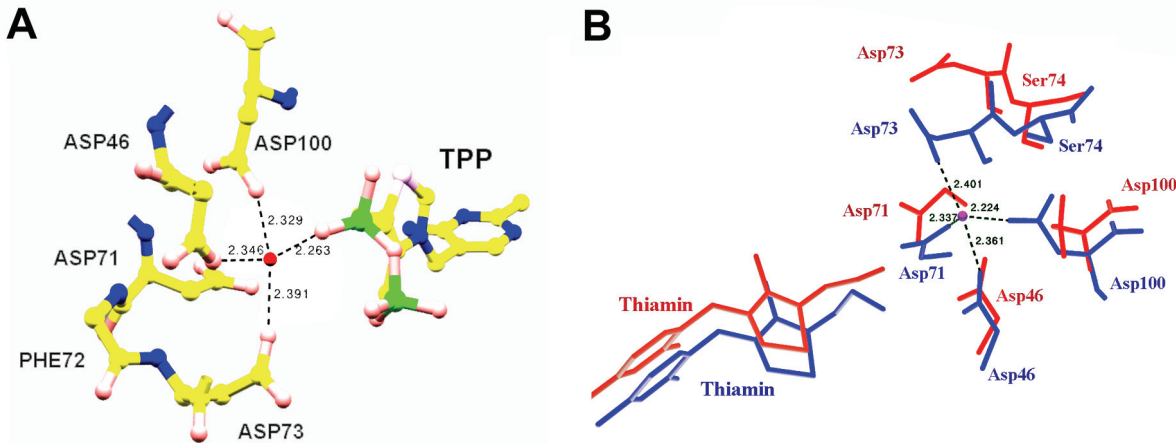


**Figure 4.** Magnesium binding in tetrameric TPP-Mg and thiamin-Mg structure complex. **A.** Magnesium binding in TPP-Mg mouse TPK complex. Magnesium coordinates with the  $\alpha$ -phosphate of TPP and Asp 46, 71 and 73. **B.** Superposition of thiamin molecules and residues surrounding magnesium ion of the dimeric (in green) and tetrameric (in red) structure. Magnesium ion binds to the enzyme via coordination with Asp 46, 71, 73 and 100. The hydroxyl group of thiamin shifted and the hydrogen bond, which used to exist between the hydroxyl group of thiamin and Asp71 in the dimeric structure, is abolished in the tetrameric structure. Distance is shown in angstrom.

cent to the pyrophosphate group of TPP in three subunits (**Figure 4A**). It coordinates with the carboxyl group of Asp46, Asp73, Asp100, and the phosphate group of TPP. However, no electron density can be assigned to MgAMP with certainty.

In the crystal structure yielded by soaking crystals with thiamin and MgAMPCPP, electron density for thiamin and  $Mg^{2+}$  are also identified (**Figure 4B**). The ring systems of thiamin bind to the protein in a similar way as that of thiamin in the dimer structure. However, the hydroxyl group of thiamin turned away from the side chain of Asp71.  $Mg^{2+}$  interacts with the protein by its coordination with the side chains of Asp 46, Asp 71, Asp73 and Asp100. The binding of  $Mg^{2+}$  reorganized the conformation of the side chains of these four Asp residues in the tetramer structure as shown in **Figure 4B**. The movement of the hydroxyl group of thiamin and that of the side chain of Asp71 abolished the hydrogen bond between them that used to exist in the dimeric structure complexed with thiamin only. Similarly, no electron density can be assigned to AMPCPP with certainty.

## Discussion

A new crystal form of P2<sub>1</sub> was yielded. TPP- $Mg^{2+}$  and thiamin- $Mg^{2+}$  complexed mouse TPK

structure were consequently solved by soaking experiments with this new crystal form. In these structures, two dimeric units of mouse TPK occupy the asymmetric units and mouse TPK associates as a tetramer, which is different from the previously described dimeric structure.

Although we cannot rule out the possibility that the tetrameric structure is an artifact from crystallographic packing, it is also possible that the tetrameric structure is a new higher order of oligomeric status of mouse TPK and it could be physiologically relevant. Firstly, the buried surface area between the two dimers is more than 3000  $\text{\AA}^2$  and occupies about 18% of the total surface area of a dimer. The area of the buried surface and the number of hydrogen bonds indicates a moderate affinity between the two dimers [17]. Secondly, the active site of the tetramer mouse TPK appears to be more closed and can potentially provide specific interactions between the side chain of Glu57 and the adenine ring of ATP. This specific interaction between an oxygen of the protein and the N6 atom of nucleotide can be found in all protein kinases and small molecule kinases, but is missing in the dimeric ternary structure of mouse TPK. Sequence analysis shows that Glu57 is conserved in human and mouse TPK and, is replaced by an Asp in yeast. It is possible that ATP binding favors the tetramer equilibrium because

the binding may introduce two extra hydrogen bonds between the N6 atom of ATP and Glu57 of the opposite dimer unit due to protein symmetry. Beside mouse TPK, it has been shown that the binding of MgATP promotes the dimerization of MalK, the ATPase component of the maltose transporter in *E. coli* previously [18].

The potential hydrogen bond between ATP and Glu57 of opposing dimer may help lower the high  $K_m$  between mouse TPK and ATP. Mouse TPK has been characterized with high  $K_m$  for ATP and low kinase activity by in vitro kinetic studies [6-8]. In good agreement, our dimeric ternary structure of mouse TPK shows that the ligand-binding groove lacks for specific interactions between the protein and the adenine ring of the nucleotide and is exposed to the solvent. However, it has been reported that thiamin is converted into TPP very rapidly in vivo [19] and free thiamin is maintained to be about 5-7% of total thiamin content in tissues [20]. Therefore, the high  $K_m$  and low specific activity characterized in vitro may not reflect the in vivo activity of TPK. It is tempting to propose that there is equilibrium between dimer and tetramer mouse TPK in vivo. The dimer form could be dominant at most circumstances but has a low activity. The tetramer species of mouse TPK may have higher activity by having a lower  $K_m$  for ATP and a higher catalytic efficiency. The activity of mouse TPK could be regulated in vivo via the oligomeric state transition. It is possible that some factors, e.g. phosphorylation on certain residue, can promote the activity of this enzyme by expediting the tetramer formation. This model of co-exists of dimer and tetramer mouse TPK appears to be supported as well by our analytical ultracentrifuge experiment done with 1mg/mL his-tag cleaved mouse TPK apoenzyme, which shows that about 95% exists as dimer and 5% exists as tetramer (data not shown). In addition, TPK has been reported to exist as both a dimer and a tetramer previously. Sanemori and Kawasaki reported both dimer and tetramer states of TPK [21]. Rat kidney TPK has also been reported to behave as a tetramer with positive cooperativity [22]. Therefore, it is possible that the activity of mouse TPK is regulated by its oligomeric status.

**Please address correspondence to:** Jing-Yuan Liu, PhD, Department of Pharmacology and Toxicology, Indiana University School of Medicine, MS550, 635 Barnhill Dr., Indianapolis, IN 46202, USA. Tel: (317) 274-7645; Fax: (317) 274-7714; E-mail

jliu2@iupui.edu

## References

- [1] Ishii K, Sarai K, Sanemori H and Kawasaki T. Concentrations of thiamine and its phosphate esters in rat tissues determined by high-performance liquid chromatography. *J Nutr Sci Vitaminol (Tokyo)* 1979; 25: 517-523.
- [2] Kimura M and Itokawa Y. Determination of thiamin and thiamin phosphate esters in blood by liquid chromatography with post-column derivatization. *Clin Chem* 1983; 29: 2073-2075.
- [3] Bettendorff L, Peeters M, Wins P and Schoffeniels E. Metabolism of thiamine triphosphate in rat brain: correlation with chloride permeability. *J Neurochem* 1993; 60: 423-434.
- [4] Shikata H, Egi Y, Koyama S, Yamada K and Kawasaki T. Properties of the thiamin triphosphate-synthesizing activity catalyzed by adenylyl kinase (isoenzyme 1). *Biochem Int* 1989; 18: 943-949.
- [5] Nosaka K, Kaneko Y, Nishimura H and Iwashima A. A possible role for acid phosphatase with thiamin-binding activity encoded by PHO3 in yeast. *FEMS Microbiol Lett* 1989; 51: 55-59.
- [6] Peterson JW, Gubler CJ and Kuby SA. Partial purification and properties of thiamine pyrophosphokinase from pig brain. *Biochim Biophys Acta* 1975; 397: 377-394.
- [7] Clark J, Gubler, Fleming G and Kuby SA. Thiamin pyrophosphokinase (ATP thiamin pyrophosphotransferase) E.C. 2.7.6.2: Purification, properties and function. In: Bisswanger H, Schellenberger A, editors. *Biochemistry and Physiology of Thiamin Diphosphate Enzyme*. Prien: Intemann; 1996. p. 557-569.
- [8] Egi Y, Koyama S, Shioda T, Yamada K and Kawasaki T. Identification, purification and reconstitution of thiamin metabolizing enzymes in human red blood cells. *Biochim Biophys Acta* 1992; 1160: 171-178.
- [9] Nosaka K, Onozuka M, Kakazu N, Hibi S, Nishimura H, Nishino H and Abe T. Isolation and characterization of a human thiamine pyrophosphokinase cDNA. *Biochim Biophys Acta* 2001; 1517: 293-297.
- [10] Timm DE, Liu J, Baker LJ and Harris RA. Crystal structure of thiamin pyrophosphokinase. *J Mol Biol* 2001; 310: 195-204.
- [11] Liu JY, Timm DE, Harris RA and Hurley TD. Studies in the structure and function of thiamin pyrophosphokinase. In: Patel MS, Jordan F, editors. *Thiamine: Catalytic mechanism and role in normal and disease states*. New York: Marcel Dekker; 2002. p.
- [12] Liu JY, Timm DE and Hurley TD. Pyridithiamine as a substrate for thiamine pyrophosphokinase. *J Biol Chem* 2006; 281: 6601-6607.
- [13] Otwinowski Z and Minor W. Processing of X-ray Diffraction Data Collected in Oscillation Mode. In: editors. *Methods in Enzymology*. Academic

# A new crystal form of mouse thiamin pyrophosphokinase

- Press; 1997. p. part A, p. 307-326.
- [14] 4. CCPN. The CCP4 suite: programs for protein crystallography. *Acta Crystallographica* 1994; D50: 760-763.
- [15] Brunger AT, Adams PD, Clore GM, DeLano WL, Gros P, Grosse-Kunstleve RW, Jiang JS, Kuszewski J, Nilges M, Pannu NS, Read RJ, Rice LM, Simonson T and Warren GL. Crystallography & NMR system: A new software suite for macromolecular structure determination. *Acta Crystallogr D Biol Crystallogr* 1998; 54 ( Pt 5): 905-921.
- [16] Janin J, Miller S and Chothia C. Surface, subunit interfaces and interior of oligomeric proteins. *J Mol Biol* 1988; 204: 155-164.
- [17] Miller S, Lesk AM, Janin J and Chothia C. The accessible surface area and stability of oligomeric proteins. *Nature* 1987; 328: 834-836.
- [18] Chen J, Lu G, Lin J, Davidson AL and Quirocho FA. A tweezers-like motion of the ATP-binding cassette dimer in an ABC transport cycle. *Mol Cell* 2003; 12: 651-661.
- [19] Tallaksen CM, Bell H and Bohmer T. The concentration of thiamin and thiamin phosphate esters in patients with alcoholic liver cirrhosis. *Alcohol Alcohol* 1992; 27: 523-530.
- [20] Rindi G, Patrini C, Comincoli V and Reggiani C. Thiamine content and turnover rates of some rat nervous regions, using labeled thiamine as a tracer. *Brain Res* 1980; 181: 369-380.
- [21] Sanemori H and Kawasaki T. Purification and properties of thiamine pyrophosphokinase in *Paracoccus denitrificans*. *J Biochem (Tokyo)* 1980; 88: 223-230.
- [22] Artsukovich IM, Voskoboev AI and Ostrovskii lu M. [Purification and several properties of thiamine pyrophosphokinase from rat liver]. *Vopr Med Khim* 1977; 23: 203-210.